

Supporting Information for

**Carbon Quantum Dot-Based Fluorescent Vesicles and Chiral Hydrogels
with Biosurfactant and Biocompatible Small Molecules**

*Xiaofeng Sun, Guihua Li, Yanji Yin, Yiqiang Zhang and Hongguang Li**

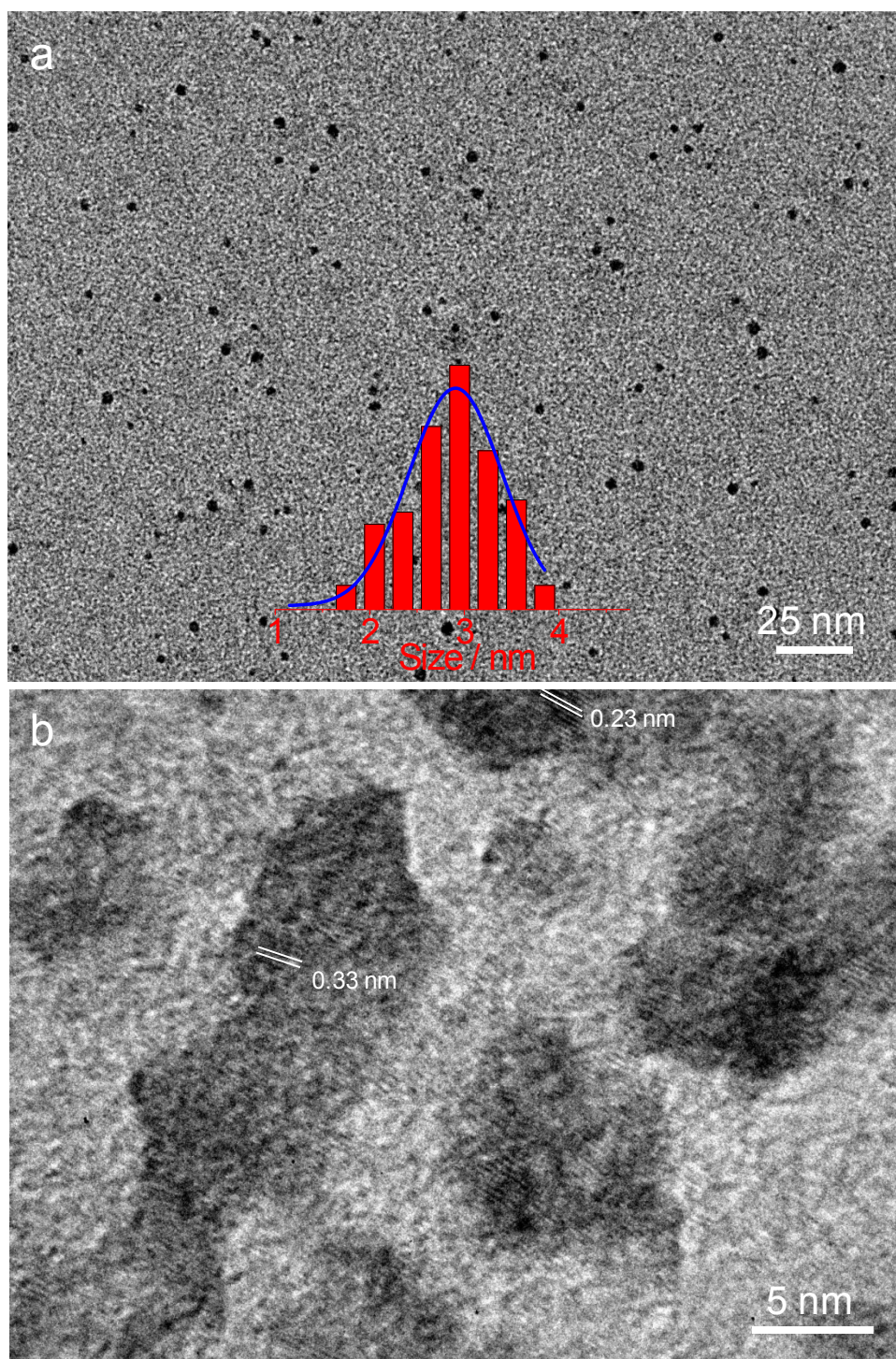


Fig. S1 (a) HR-TEM image and the size distribution of as-prepared CQDs. (b) Typical single CQDs with lattice parameters of 0.23 nm and 0.33 nm, respectively.

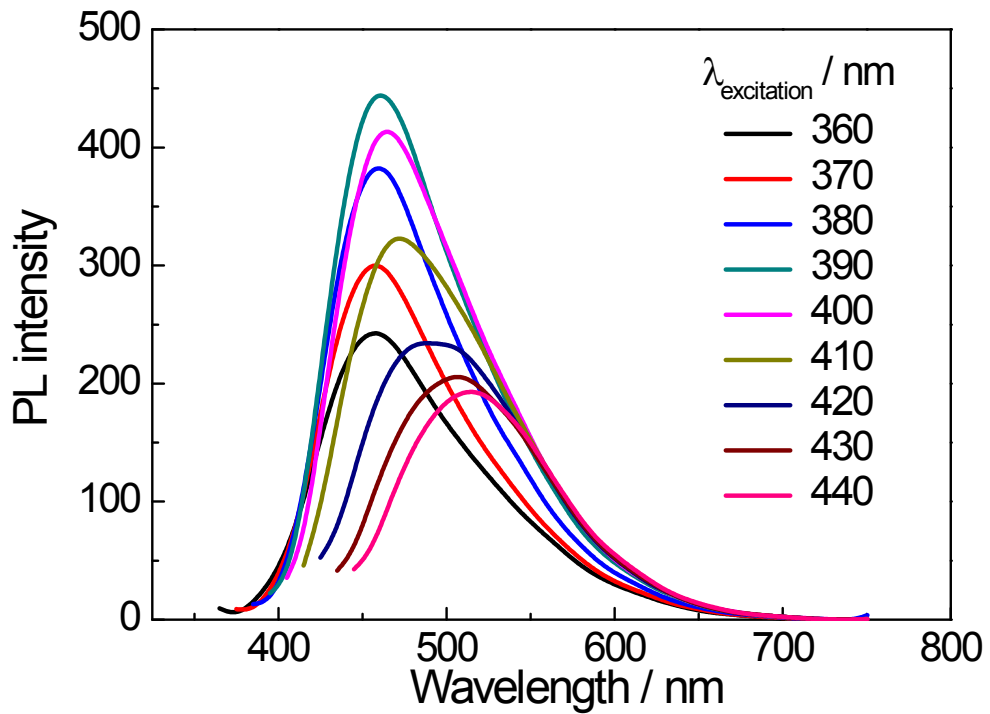


Fig. S2 Emission spectra at varying excitation wavelengths of the CQDs aqueous solution ($0.5 \text{ mg}\cdot\text{mL}^{-1}$).

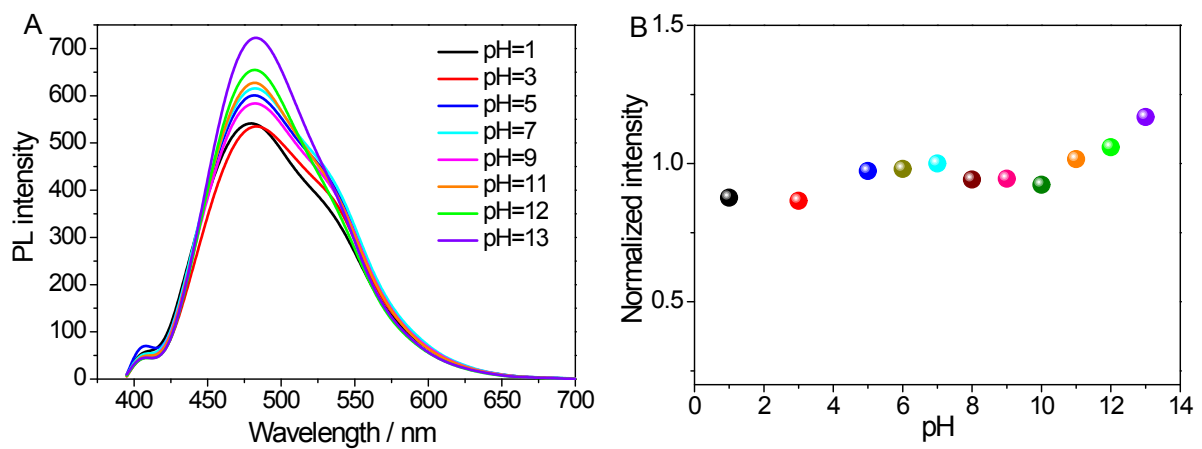


Fig. S3 A) Emission spectra at $\lambda_{\text{ex}}=470 \text{ nm}$ as a function of pH. B) Variation of the PL intensity at $\lambda_{\text{ex}}=470 \text{ nm}$ as a function of pH ($0.5 \text{ mg}\cdot\text{mL}^{-1}$).

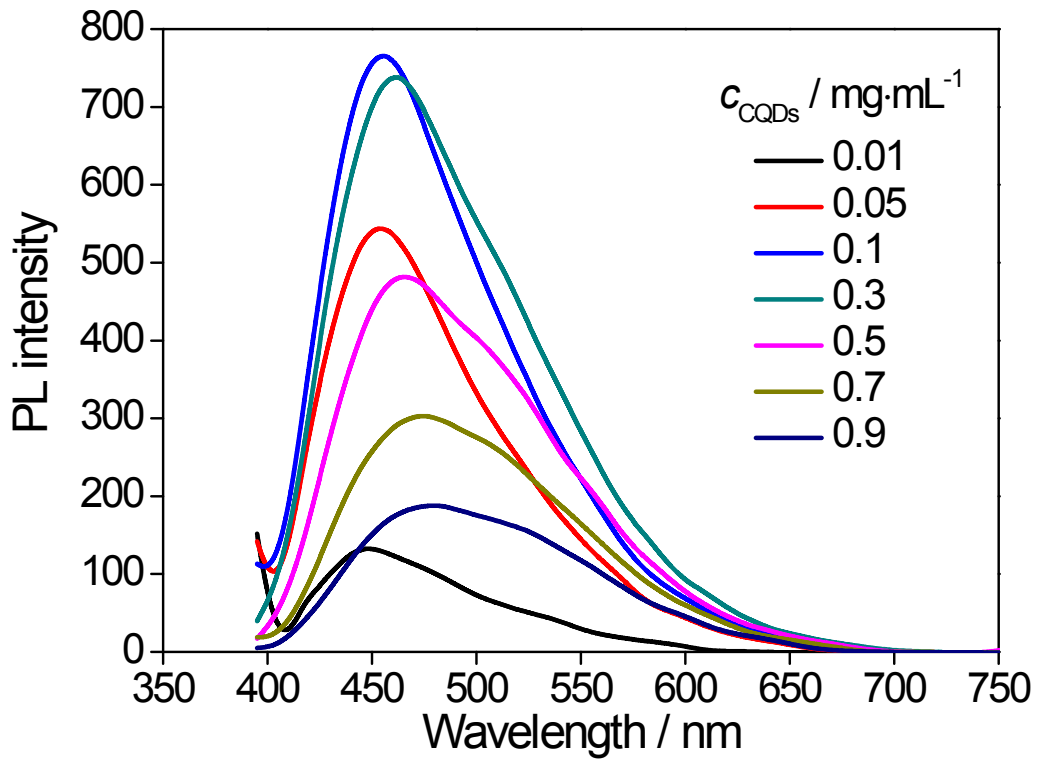


Fig. S4 Emission spectra at $\lambda_{\text{ex}} = 390 \text{ nm}$ as a function of c_{CQDs} .

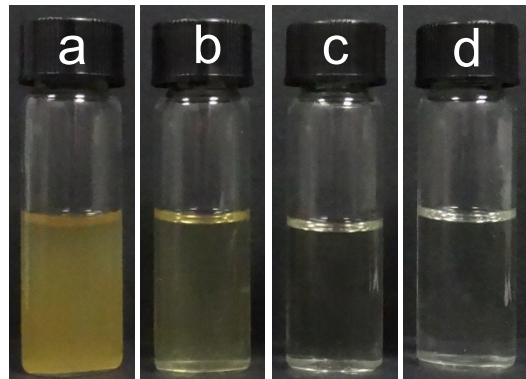


Fig. S5 Photos of the aqueous solutions containing a) $0.5 \text{ mg}\cdot\text{mL}^{-1}$ CQDs / $1.0 \text{ mmol}\cdot\text{L}^{-1}$ NaDC; b) $0.25 \text{ mg}\cdot\text{mL}^{-1}$ CQDs / $0.5 \text{ mmol}\cdot\text{L}^{-1}$ NaDC; c) $0.1 \text{ mg}\cdot\text{mL}^{-1}$ CQDs / $0.20 \text{ mmol}\cdot\text{L}^{-1}$ NaDC; d) $0.05 \text{ mg}\cdot\text{mL}^{-1}$ CQDs / $0.1 \text{ mmol}\cdot\text{L}^{-1}$ NaDC.

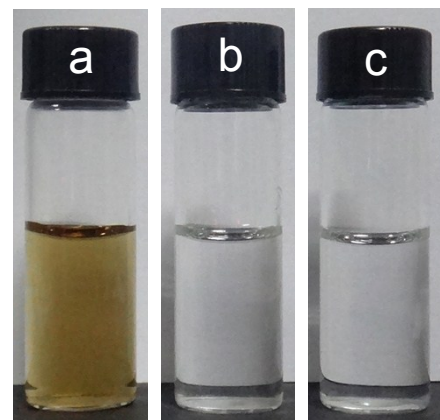


Fig. S6 Photos of the aqueous solutions containing a) $0.5 \text{ mg}\cdot\text{mL}^{-1}$ CQDs, b) $1.0 \text{ mmol}\cdot\text{L}^{-1}$ NaDC and c) $8.0 \text{ mmol}\cdot\text{L}^{-1}$ NaDC.

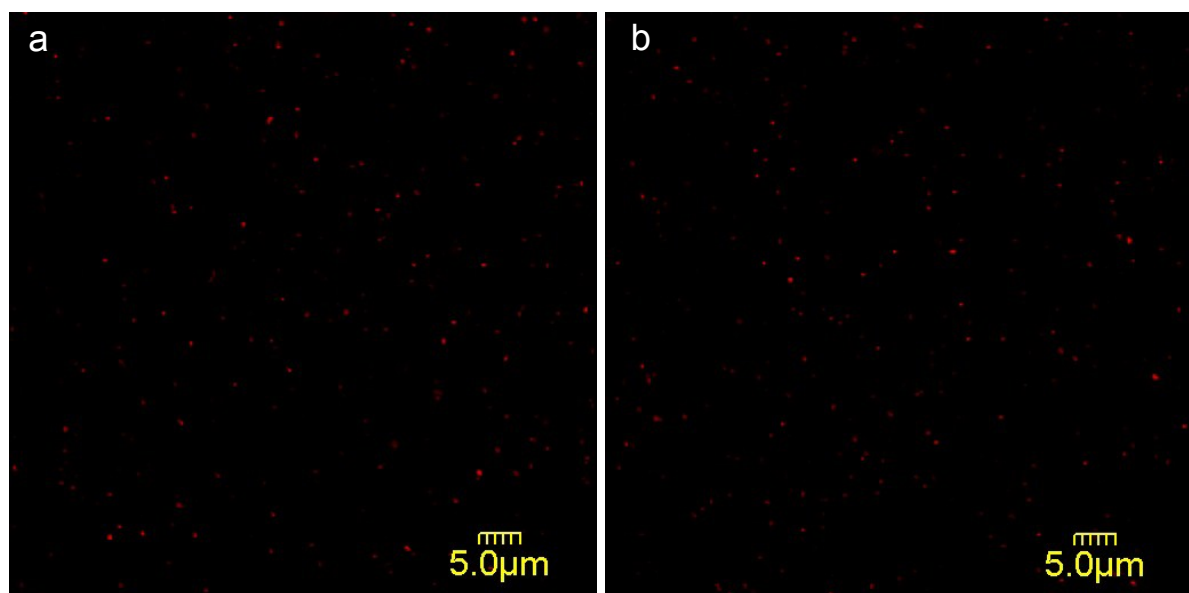


Fig. S7 Confocal fluorescence micrographs of the vesicles formed in the sample

containing 1.0 (a) and 8.0 mmol·L⁻¹ NaDC (b). $c_{\text{CQDs}} = 0.5 \text{ mg} \cdot \text{mL}^{-1}$.

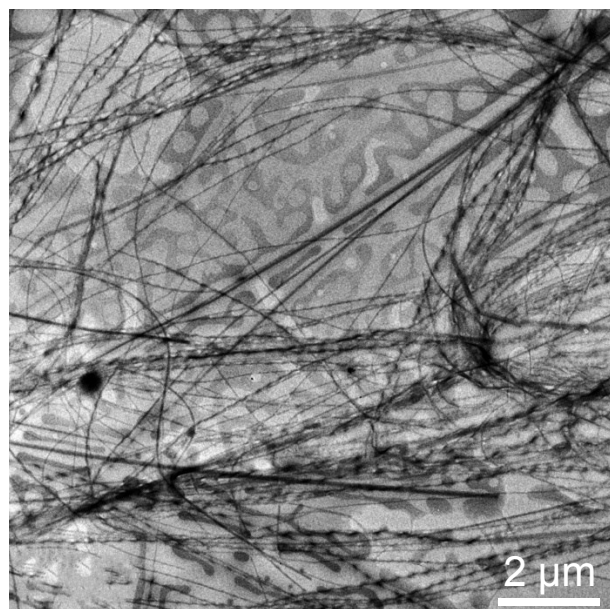


Fig. S8 TEM image at lower magnification compared to that shown in the maintext (Fig. 4b)

of the hydrogel formed at 100 mmol·L⁻¹ NaDC, 0.5 mg·mL⁻¹ CQDs and 50 mmol·L⁻¹ GSH.

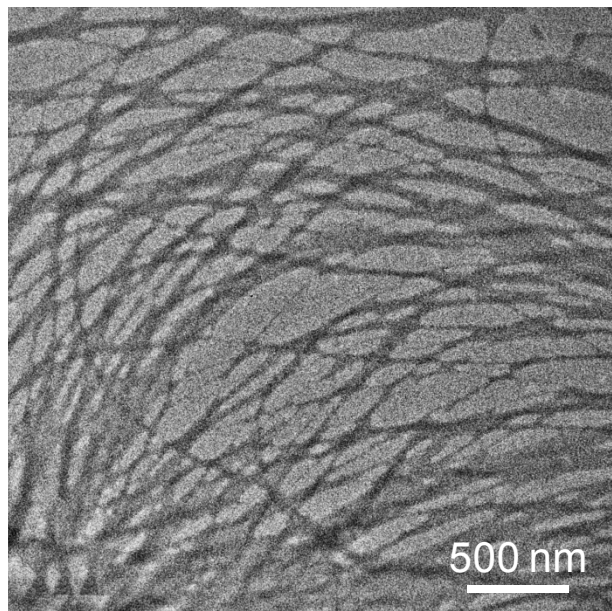


Fig. S9 TEM image of the hydrogel formed at $100 \text{ mmol}\cdot\text{L}^{-1}$ NaDC and $50 \text{ mmol}\cdot\text{L}^{-1}$ GSH without CQDs.

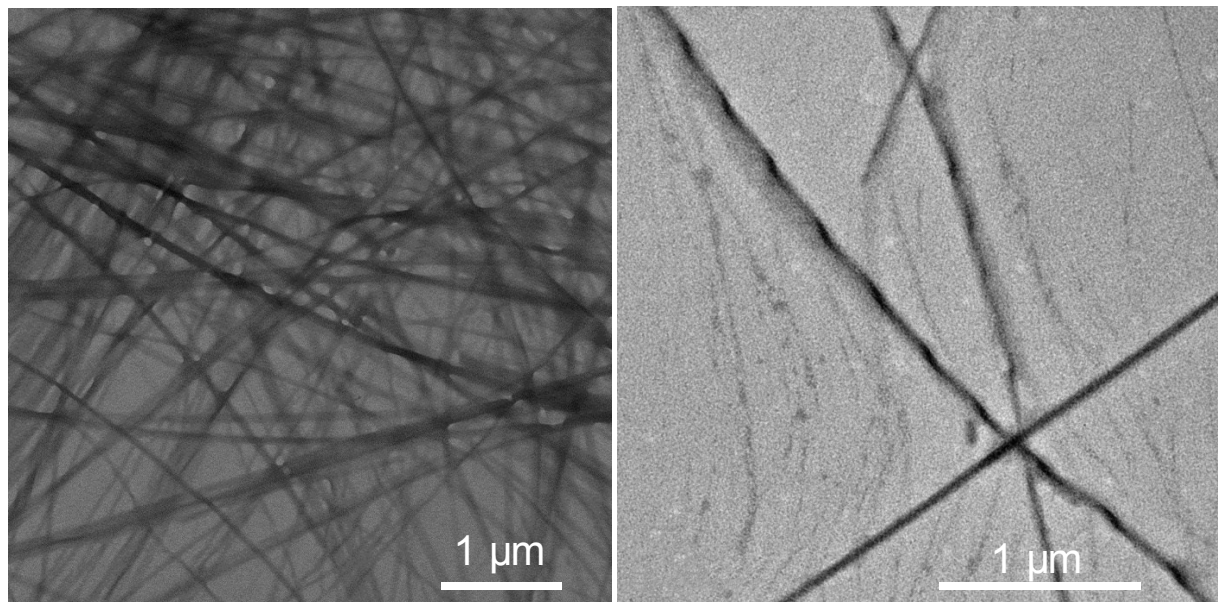


Fig. S10 TEM images at different magnifications of the hydrogel formed at $100 \text{ mmol}\cdot\text{L}^{-1}$ NaDC and $60 \text{ mmol}\cdot\text{L}^{-1}$ GSH without CQDs.

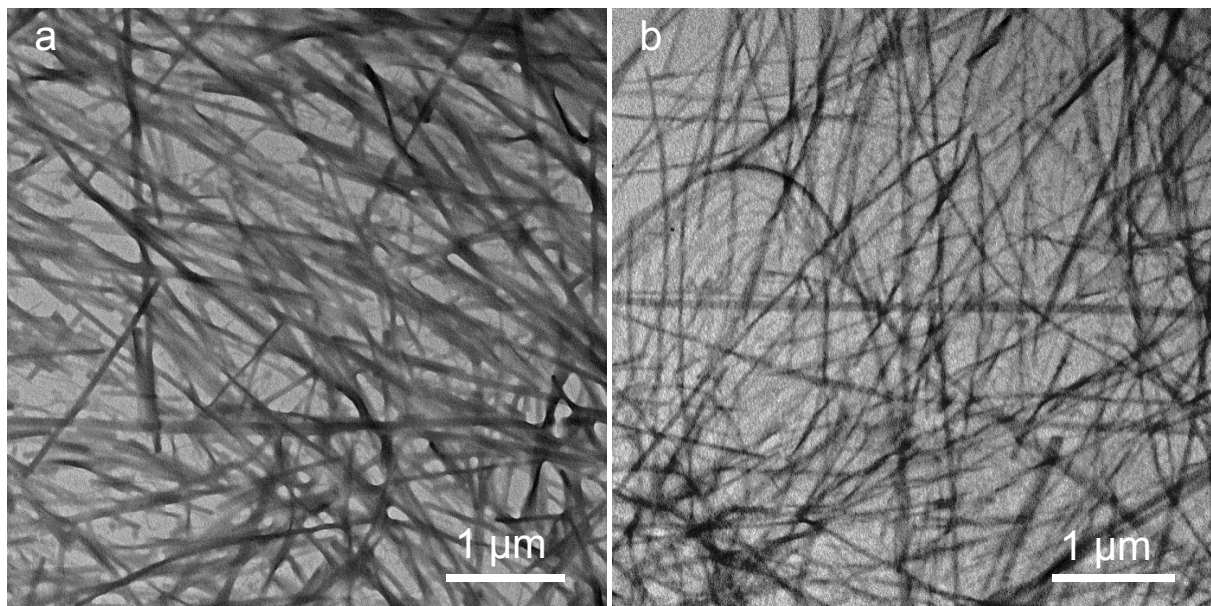


Fig. S11 TEM images of the hydrogels formed at $100 \text{ mmol}\cdot\text{L}^{-1}$ NaDC and $80 \text{ mmol}\cdot\text{L}^{-1}$ GSH without (a) and with (b) $0.5 \text{ mg}\cdot\text{mL}^{-1}$ CQDs.

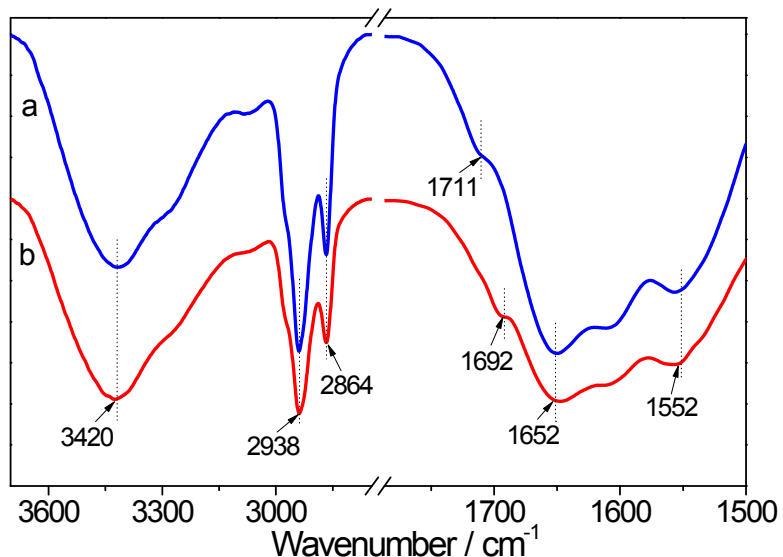


Fig. S12 FTIR spectra of the hydrogel containing $100 \text{ mmol}\cdot\text{L}^{-1}$ NaDC and $50 \text{ mmol}\cdot\text{L}^{-1}$ GSH without (curve a) and with (curve b) $0.5 \text{ mg}\cdot\text{mL}^{-1}$ CQDs.

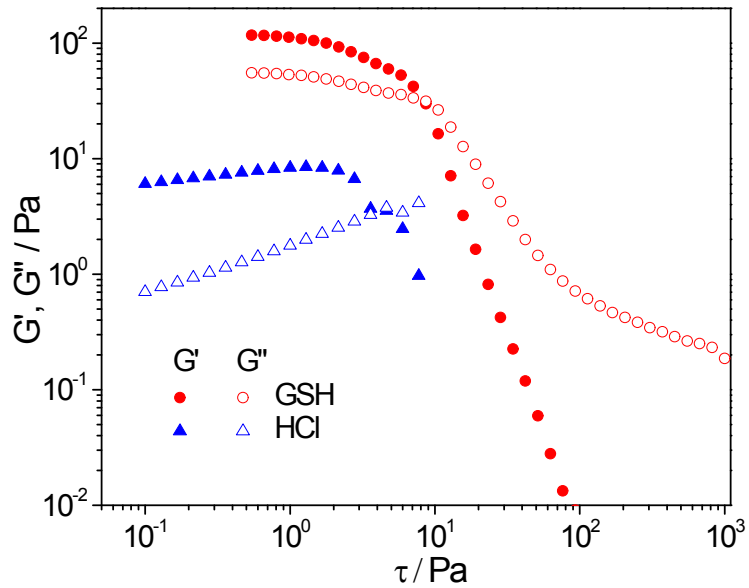


Fig. S13 Stress sweep of the hydrogels with constant c_{NaDC} ($100 \text{ mmol}\cdot\text{L}^{-1}$) and c_{CQDs} ($0.5 \text{ mg}\cdot\text{mL}^{-1}$) with $30 \text{ mmol}\cdot\text{L}^{-1}$ GSH and HCl ($\text{pH} = 7$).

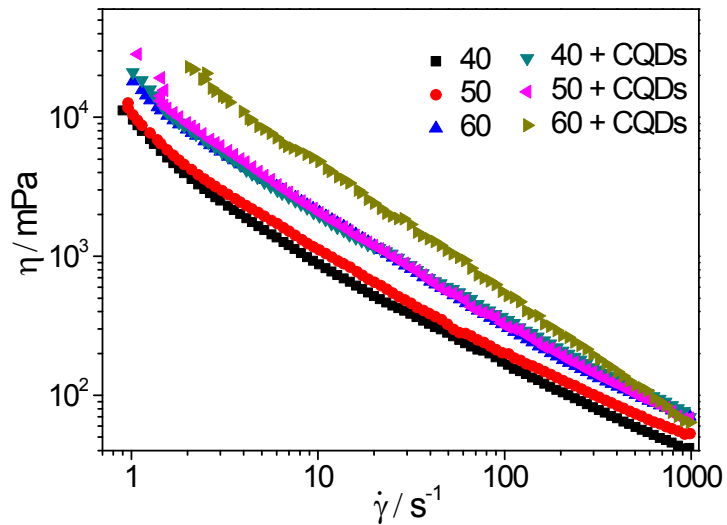


Fig. S14 Variation of the viscosity as a function of shear rate in steady-state shear measurements of the hydrogels with $100 \text{ mmol}\cdot\text{L}^{-1}$ NaDC and varying amount of GSH ($\text{mmol}\cdot\text{L}^{-1}$) as indicated without and with $0.5 \text{ mg}\cdot\text{mL}^{-1}$ CQDs.

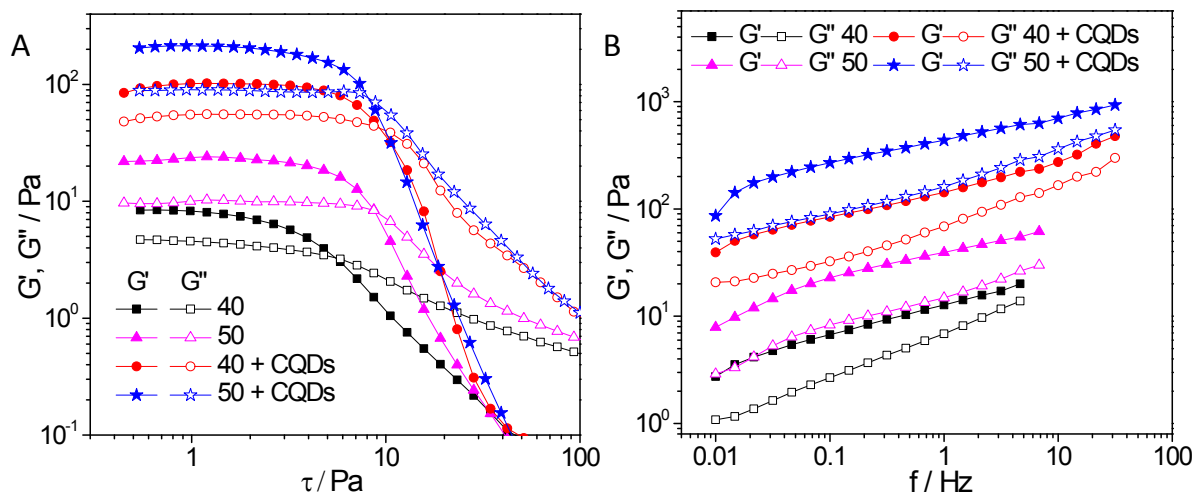


Fig. S15 Rheological properties of the hydrogels with constant c_{NaDC} ($100 \text{ mmol}\cdot\text{L}^{-1}$) and c_{GSH} (40 or $50 \text{ mmol}\cdot\text{L}^{-1}$) without and with $0.5 \text{ mg}\cdot\text{mL}^{-1}$ CQDs as indicated. A) Stress sweep at a constant frequency of 1.0 Hz . B) Frequency sweep at a constant stress of 1.0 Pa .

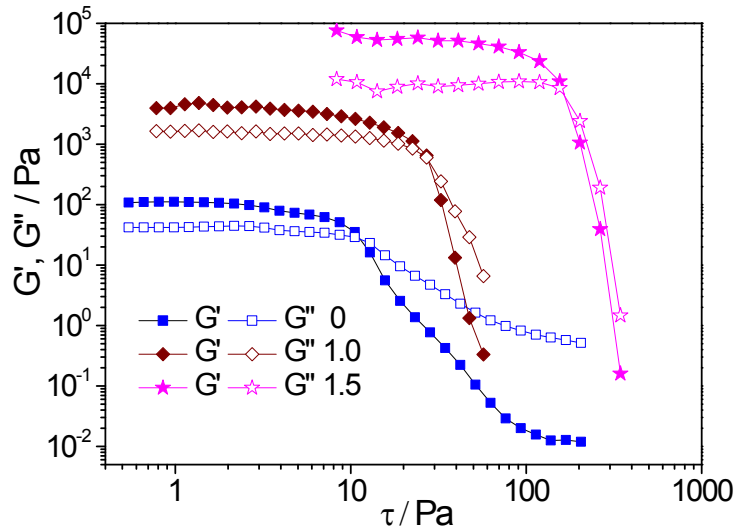


Fig. S16 Stress sweep of the hydrogels with constant c_{NaDC} ($100 \text{ mmol}\cdot\text{L}^{-1}$) and c_{GSH} ($60 \text{ mmol}\cdot\text{L}^{-1}$) but different c_{CQDs} ($\text{mg}\cdot\text{mL}^{-1}$) as indicated ($f = 1.0 \text{ Hz}$).

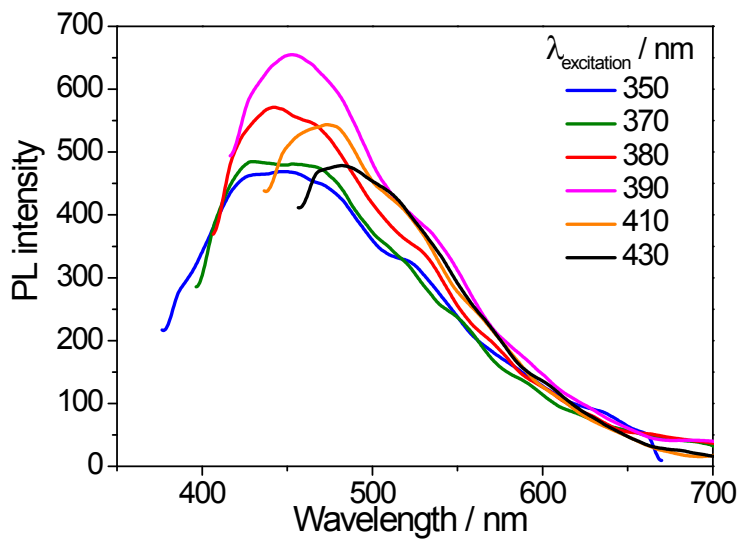


Fig. S17 Wavelength-dependent photoluminescence of the xerogel containing $100 \text{ mmol}\cdot\text{L}^{-1}$ NaDC, $0.5 \text{ mg}\cdot\text{mL}^{-1}$ CQDs and $40 \text{ mmol}\cdot\text{L}^{-1}$ GSH.

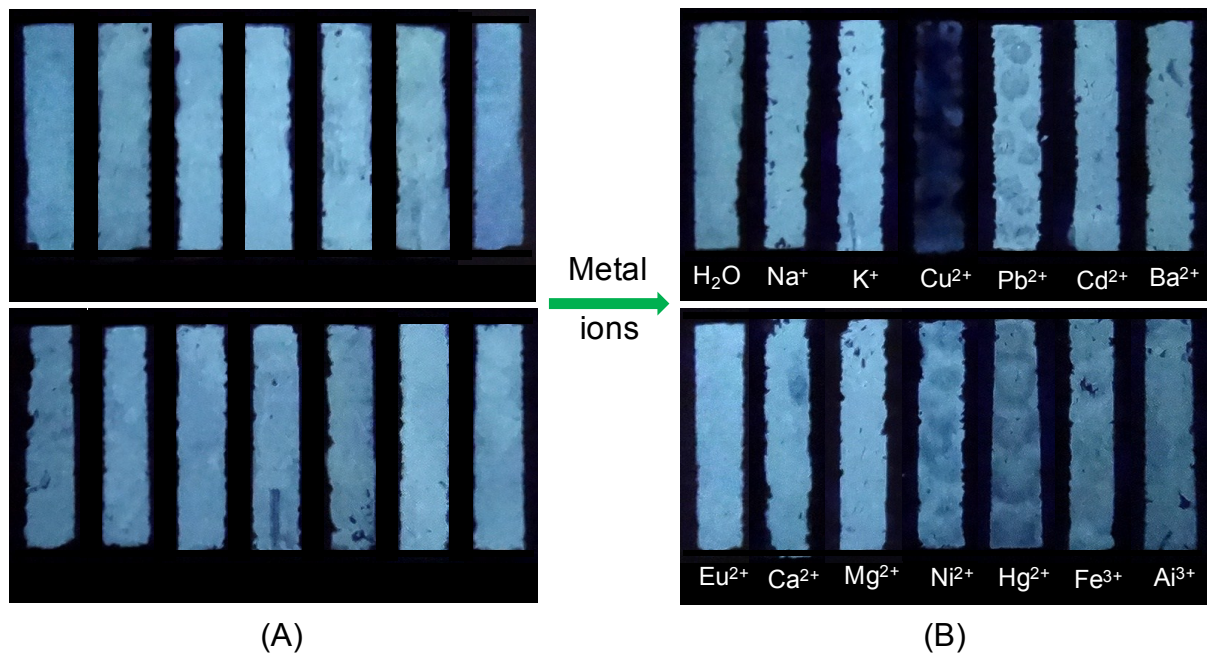


Fig. S18 Visual detection of metal ions using the silica gel plate coated by hydrogel containing c_{NaDC} ($100 \text{ mmol}\cdot\text{L}^{-1}$) / c_{CQDs} ($0.5 \text{ mg}\cdot\text{mL}^{-1}$) / c_{GSH} ($40 \text{ mmol}\cdot\text{L}^{-1}$) in the absence (A) and presence of metal ions (B, $2 \text{ mmol}\cdot\text{L}^{-1}$), respectively. The photos were taken under a 254 nm UV lamp.

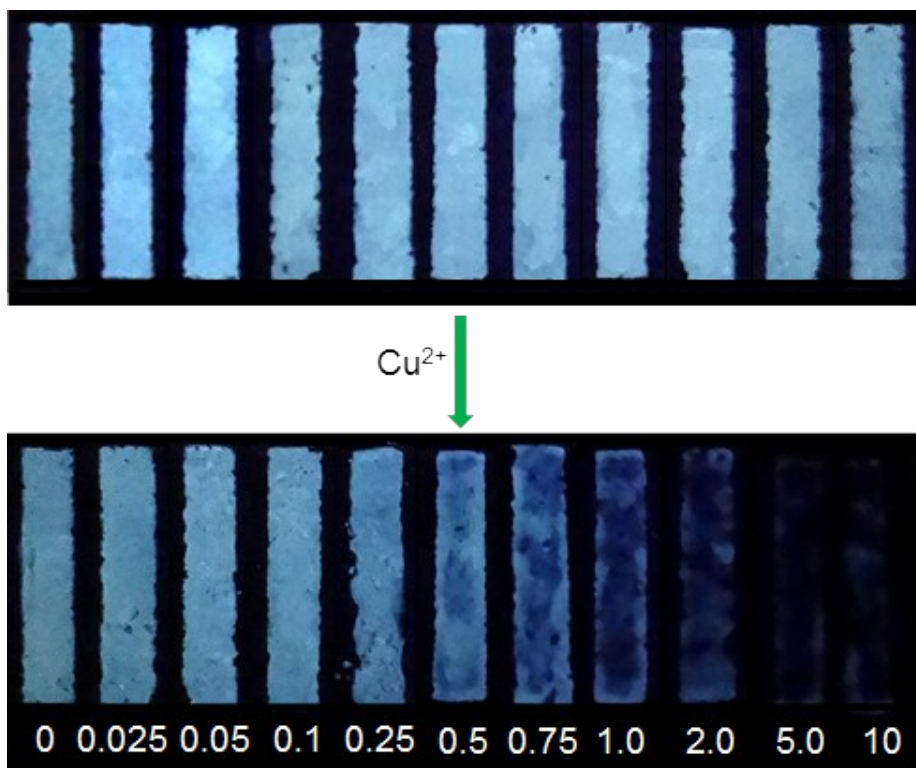


Fig. S19 Visual detection of Cu^{2+} using the silica gel plate coated by hydrogel containing 100 $\text{mmol}\cdot\text{L}^{-1}$ NaDC, 0.5 $\text{mg}\cdot\text{mL}^{-1}$ CQDs and 40 $\text{mmol}\cdot\text{L}^{-1}$ GSH. The photos were taken under a 254 nm UV lamp.

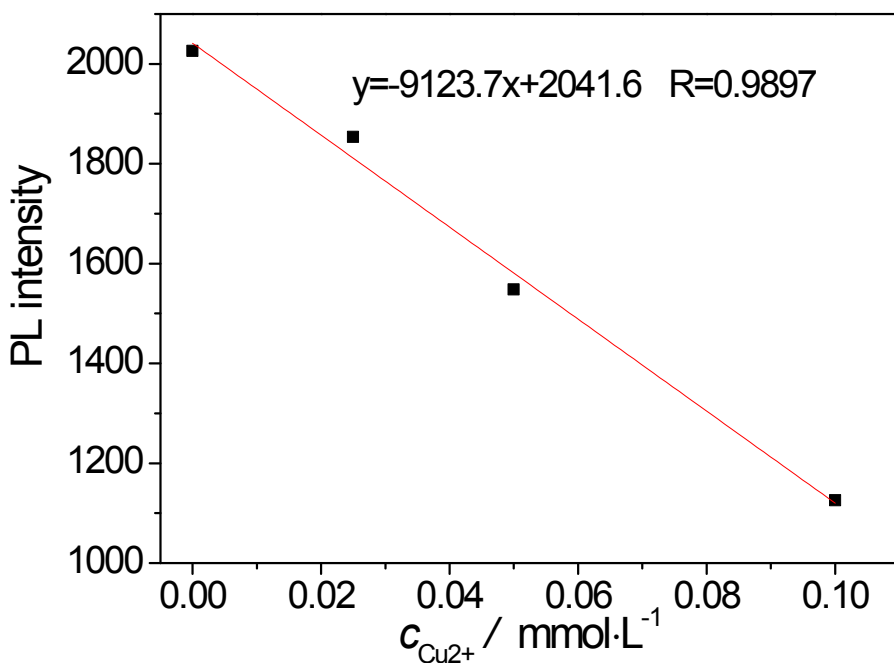


Fig. S20 The PL intensity as a function of $c_{\text{Cu}^{2+}}$ (light red line is a linear fitted curve of points).